Journal of Applied Pharmaceutical Research
Volume 13 Issue 5, Year of Publication 2025, Page 38 – 46
DOI: https://doi.org/10.69857/joapr.v13i5.1668

Check for updates

Research Article

JOURNAL OF APPLIED PHARMACEUTICAL RESEARCH | JOAPR
www.japtronline.com ***ISSN: 2348 – 0335***

DESIGN, FORMULATION, AND EVALUATION OF HYDROGEL NETWORK BASED MICROBEADS FOR PROLONGED RELEASE OF VALACYCLOVIR

Sankar Narayan Bhunia[1,2], Dipankar Saha[2]*, Sudipta Das[2], Rimi Dey[2], Sawan Das[2]

Article Information
Received: 22nd June 2025
Revised: 14th September 2025
Accepted: 6th October 2025
Published: 31st October 2025

Keywords
Valacyclovir hydrochloride, hydrogel microbeads, gellan gum, sodium alginate, ionic gelation.

ABSTRACT
Background: This study aimed to formulate and develop hydrogel network-based microbeads for the prolonged release of the antiviral drug Valacyclovir, focusing on the effect of natural gum/polymer ratios in their preparation. **Methodology:** Microbeads containing Valacyclovir hydrochloride were prepared using the ionotropic gelation method, which involved sodium alginate and gellan gum as the polymers, and aluminum chloride as the crosslinking agent. **Result:** In the evaluation, the F1 batch exhibited the highest swelling capacity, drug entrapment efficiency, and drug release profile. Across all formulations, the particles were round to oval in shape, with sizes ranging from 598 to 816µm. Drug release kinetics revealed that the Higuchi model best explained the formulations. The surface morphology of the best-performing formulation was examined using scanning electron microscopy (SEM). **Discussion:** The findings proposed that the prepared microbeads function as swellable matrix-type systems, enabling prolonged drug delivery. The Higuchi model fit supported a diffusion-controlled release mechanism, while the SEM analysis confirmed the suitability of the microbead structure for sustained release applications. **Conclusion:** These kinds of ionotropically-gelled alginate-based microbeads may improve patient compliance by reducing dosing frequency and enhancing oral bioavailability.

INTRODUCTION

Microbeads are small, free-flowing, spherical shapes with a particle diameter range of 1 to 1000 µm. They are typically composed of a mixture of drug and polymer solutions. In a controlled drug delivery system, microbeads are called drug carriers [1]. Nowadays, microbeads are widely used as microparticles in controlled or prolonged drug delivery systems to enhance drug delivery, maintain effectiveness, and improve bioavailability [2-3]. Hydrogel-based microbeads have garnered considerable interest as carriers for controlled or sustained oral drug delivery due to their high-water content, modifiable structure, and biocompatibility. These systems provide a three-dimensional network capable of encapsulating therapeutic agents and enabling prolonged release through swelling and diffusion mechanisms. Among natural polymers, sodium alginate and gellan gum have been widely studied for their synergistic potential in forming stable hydrogel matrices [4-5]. Valacyclovir hydrochloride, a prodrug of acyclovir, exhibits an oral bioavailability of approximately 55% and a short biological

[1]*School of Pharmacy, Girijananda Chowdhury University, Guwahati, Assam, 781017, India.*
[2]*Department of Pharmaceutics, Netaji Subhas Chandra Bose Institute of Pharmacy, Chakdaha, 741222, Nadia, West Bengal, India.*

For Correspondence: **saha.deep.ghy@gmail.com**

half-life of 2.5–3 hours, necessitating frequent administration to maintain therapeutic levels. This often leads to poor patient adherence and suboptimal therapeutic outcomes. Therefore, the development of a sustained-release microbead system becomes a crucial strategy to enhance therapeutic efficiency and compliance [6-7]. Ionic gelation, the technique used in this study, is a mild, aqueous-based method in which cross-linking occurs through the interaction of multivalent cations, such as aluminum (Al^{3+}), with anionic polymers like alginate. This process produces uniform, stable microbeads under gentle conditions, making it suitable for labile drugs [8-0]. Hydrogels [11], particularly those derived from biocompatible natural polymers, have emerged as promising platforms for prolonged-release formulations. Their high-water content & 3-dimensional polymeric network facilitate not only drug encapsulation but also prolonged drug release. Sodium alginate, a linear anionic polysaccharide, forms ionically cross-linked gels in the presence of multivalent cations, such as aluminum (Al^{3+}), resulting in robust hydrogel matrices. Gellan gum, a highly viscous polysaccharide, can synergistically enhance gel strength and modulate drug release when used in combination with alginate. The present study addresses these challenges by employing a drug-polymer hydrogel system, consisting of sodium alginate and gellan gum, crosslinked with aluminum chloride at two concentrations (1% and 2%). The objective is to examine the influence of selected variables on the formation, structural integrity, and drug release characteristics of Valacyclovir-loaded microbeads, ultimately enabling the design of a reliable and effective prolonged-release formulation.

MATERIALS AND METHODS

Valacyclovir, Sodium Alginate, and Gellan gum were purchased from Yarrow Chem Products, Mumbai, and Aluminium Chloride was collected from Loba Chemie Pvt. Ltd., Mumbai. All reagents used were of analytical grade. No human or animal subjects were used in this study.

Preparation of Microbeads

Microbeads were prepared using the ionic gelation technique, and formulation composition was provided (Table 1). Sodium alginate and gellan gum were separately dissolved in distilled water at 50 °C, and then blended at predefined ratios (1:1, 1:2, 2:1) to obtain a uniform polymer solution. Valacyclovir was incorporated into this mixture and stirred continuously for 30 minutes to ensure homogeneity. The resulting dispersion was transferred into a 10 mL syringe fitted with a 21-gauge stainless steel needle and dropped at a controlled rate of approximately 1 mL/min into a gently stirred aluminum chloride solution (1% or 2% w/v). The crosslinking solution was maintained under magnetic stirring at 400 rpm to prevent bead aggregation. The beads were allowed to crosslink for 5 minutes at room temperature, then filtered and thoroughly rinsed with distilled water to remove excess aluminum chloride. They were subsequently dried in a hot-air oven at 40°C for 24 hours. The dried microbeads were stored in airtight containers until further evaluation [8, 12].

FORMULATION COMPOSITION

Table 1: Composition of microbeads

Ingredients	F1	F2	F3	F4	F5	F6
Valacyclovir HCl (mg)	500	500	500	500	500	500
Sodium Alginate (mg)	400	300	200	400	300	200
Gellan Gum (mg)	200	300	400	200	300	400
Aluminium Chloride (% w/v)	1%	1%	1%	2%	2%	2%

EVALUATION PARAMETERS

Percentage Yield (%): Percentage yield is calculated to evaluate the efficiency of the formulation process. It is determined based on the weight of Valacyclovir-loaded microbeads obtained relative to the total weight of the drug and polymers used. This calculation is applied to all formulations prepared using the following equation [13-14].

$$\% \textbf{ yield } = \frac{\boldsymbol{Weight\ of\ the\ microbeads\ obtained}}{\boldsymbol{Weight\ of\ the\ polymers\ and\ drug\ isused}} \times \mathbf{100}$$

Drug Entrapment Efficiency (DEE% %): DEE indicates the fraction of the drug successfully encapsulated within the beads. Approximately 50 mg of crushed beads from each formulation were dissolved in 50 mL of phosphate buffer (pH 6.8) and sonicated for 10 minutes at room temperature to ensure complete drug release, followed by filtration. The filtrate was analyzed by UV-Visible spectrophotometry at 252 nm using a calibration curve for Valacyclovir [15-17].

$$\textbf{DEE } (\%) = \frac{\boldsymbol{Experimental\ amount\ of\ drug\ present\ in\ the\ microbeads}}{\boldsymbol{Theoretical\ amount\ of\ drug\ taken\ initially}} \times \mathbf{100}$$

Swelling Index (%): The swelling behavior of the beads in aqueous media determines the capacity of the polymer matrix to absorb water, which in turn influences the drug diffusion rate. Dried microbeads (50 mg) were placed in 50 mL of phosphate

buffer (pH 6.8) at 37°C. At regular time intervals, beads were removed, gently blotted to remove excess water, and weighed [18-19].

$$\text{Swelling Index } (\%) = \frac{Wt\ of\ swelled\ microbeads - Wt\ of\ dried\ microbeads}{Weight\ of\ dried\ microbeads} \times 100$$

Particle Size Analysis: The mean diameter of microbeads was determined using a digital microscope fitted with a calibrated micrometer scale. At least 100 beads per formulation were measured to ensure statistical accuracy [20].

$$\text{Average particle size} = \frac{\sum Individual\ diameter\ of\ the\ beads}{Number\ of\ beads}$$

Surface Morphology: The surface morphology of Valacyclovir HCl-loaded microbeads was examined by Scanning Electron Microscopy (SEM). SEM has been used to determine particle size distribution and surface texture. SEM is conducted by using JEOL JSM–7500F Field Emission Scanning Electron Microscope, and the result is calculated through JED-2300 Analysis Station Software. Initially, microbeads were placed on an aluminum stub using double-sided carbon tape and coated with a silver layer. The stub was then visualized under a scanning electron microscope [21-22].

In Vitro Drug Release: Drug release studies were conducted using a USP Type II dissolution apparatus. Beads equivalent to 100 mg of Valacyclovir were placed in 900 mL of phosphate buffer (pH 6.8), maintained at 37 ± 0.5°C, and rotated at 50 rpm. At predetermined intervals, 5 mL of dissolution medium was withdrawn, filtered, and analyzed at 252 nm using a UV-Visible spectrophotometer. Each withdrawn volume was replaced with fresh buffer [23-24].

Drug Release Kinetics: The drug release pattern of microbeads depends on various factors, including size, polymer density, crosslinking agents, polarity, pH of the medium, and the rate and duration of drug release through the matrix.

Following the collection of dissolution data, the kinetics of the drug release and general release behavior via microbeads were investigated by fitting the data into established release models, including the zero-order, first-order, Higuchi, Hixon–Crowell, and Korsmeyer–Peppas models [8, 19, 25]. Several significant mathematical models were utilized to examine the in vitro drug release data kinetically [26].

$$\textbf{Zero order model}: Q_t = Q_0 + K_o t$$

$$\textbf{First order model}: log\ Q_t - \frac{K_1 t}{2.303}$$

$$\textbf{Higuchi model}: Q_t = K_H \sqrt{t}$$

$$\textbf{Korsmeyer - Peppas model}: \frac{M_t}{M_\infty} = Kt^n$$

Where: 'n' is the release exponent indicating the mechanism (Fickian or non-Fickian)

RESULTS AND DISCUSSION

This study presents a novel application of a hydrogel-based microbead system for the prolonged release of Valacyclovir Hydrochloride. The strategic combination of sodium alginate and gellan gum, with variation in aluminum chloride concentration, enabled fine-tuning of the polymeric matrix's porosity, swelling behavior, and diffusion properties. This formulation strategy, employing a dual-polymer matrix with variable ionic cross-linking, has not been previously optimized for Valacyclovir hydrochloride delivery, making a novel contribution to hydrogel-based antiviral drug delivery systems. The experimental outcomes help to understand the polymer ratio and cross-linker concentration, and they critically influence the morphology, structural integrity, and drug release behavior of the prepared hydrogel microbeads. Formulations using a higher proportion of gellan gum demonstrated improved viscosity, hydration capacity, and entrapment efficiency, likely due to gellan's extended molecular chains forming a more cohesive network with the alginate.

Selection of wavelength and standard calibration curve

The λ_{max} of Valacyclovir HCl (Figure 1) and standard calibration curve of valacyclovir was determined by using a UV-Visible Spectrophotometer [27-28].

Calibration Curve

The absorbance of Valacyclovir hydrochloride was measured at 252 nm using UV–Vis spectrophotometry. Calibration standards were prepared within the selected concentration range, and the method exhibited good linearity with the regression equation $y = 0.050x + 0.011$ ($R^2 = 0.997$).

Compatibility Studies

The compatibility between the drug and various polymers used was determined by using FTIR [28-30]. FT-IR analysis was performed using a JASCO FT-IR spectrometer. The FTIR spectra of Valacyclovir, gellan gum, and formulation F1 were analyzed for drug–polymer interactions (Figure 2-4).

Valacyclovir showed characteristic peaks for O–H/N–H stretching (~3439–3204 cm^{-1}), C–H stretching (~2966 cm^{-1}), C=O/amide groups (~1742–1679 cm^{-1}), and C–O/C–N vibrations (~1298–1122 cm^{-1}). Gellan gum displayed a broad O–H band (~3388 cm^{-1}), carboxylate groups (~1616 cm^{-1}), and C–O–C stretching (~1017 cm^{-1}). In the formulation, drug peaks were retained with slight shifts, while polymer carboxylate bands showed changes in intensity and position. The presence of the main peaks of Valacyclovir in the formulation indicates the drug remained stable and was physically entrapped in the beads. Minor shifts in polymer carboxylate bands suggest ionic interactions with cross-linker (Al^{3+}), confirming cross-linking within the hydrogel network. No new peaks appeared, indicating that there was no chemical incompatibility between the drug and the polymers.

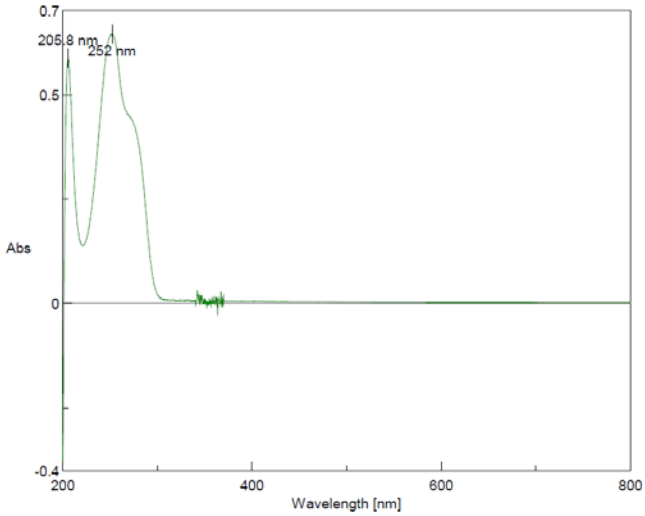

Figure 1: UV-Visible spectrum of Valacyclovir HCl showing maximum absorbance at 252 nm.

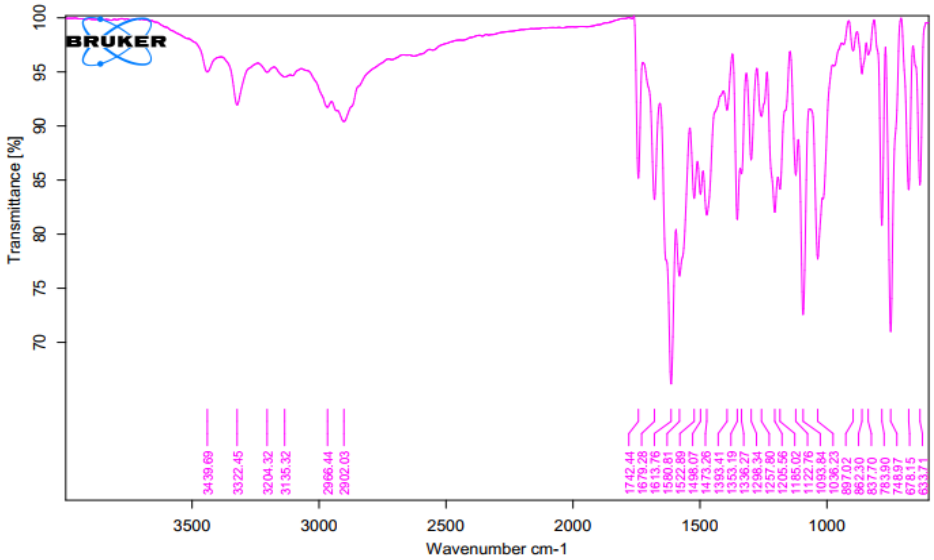

Figure 2: FTIR of Valacyclovir Hydrochloride

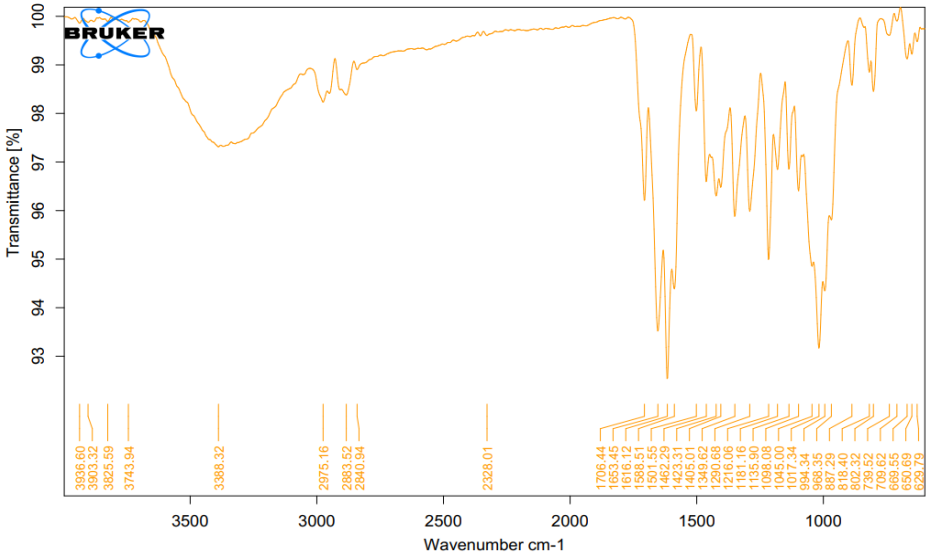

Figure 3: FTIR of Gellan Gum

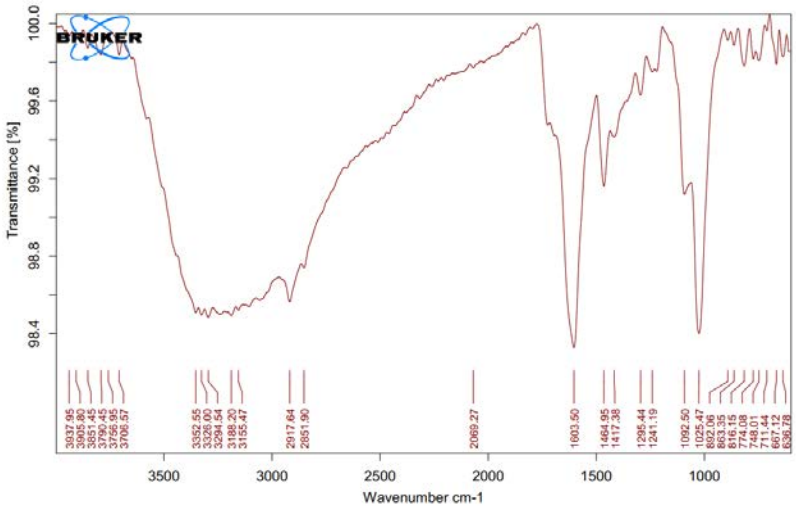

Figure 4: Drug polymer compatibility study of Formulation 1

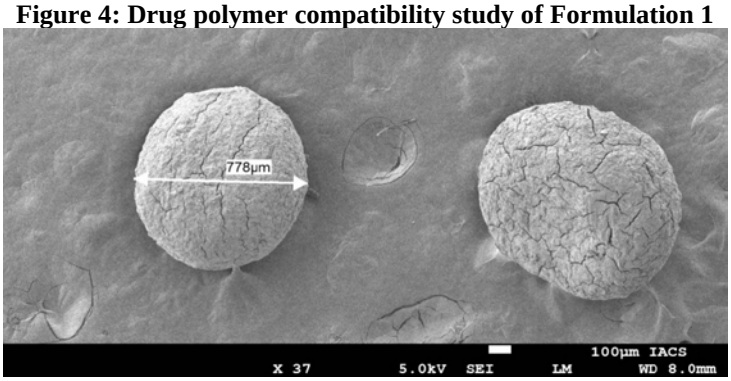

Figure 5: Scanning electron microscopy image of Valacyclovir microbeads at 37x magnification

Surface Morphology

Scanning electron microscopy (SEM) was used to examine the surface morphology. The analysis was conducted at 37x magnification, and an SEM photograph was taken at 5 kV, allowing for examination of the morphology (Figure 5). The SEM image of the prepared microbeads displayed almost spherical particles with smooth surfaces and negligible surface cracks. The average particle size was observed to be ~778 µm, reliable with the microscopic particle size analysis.

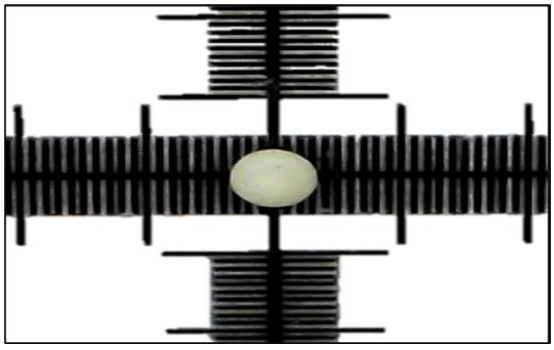

Figure 6: Particle size measurement of prepared microbeads using a digital microscope

The spherical morphology analysis confirmed successful bead formation by ionic gelation. Minor cracks on the surface are likely due to drying, but the overall smoothness suggests a compact matrix suitable for controlled drug release.

Measurement of Particle Size

The size of the particles was determined using a digital microscope, and images were captured (Figure 6). The average particle size of the formulations ranged from 598 ± 3 to 816 ± 2 µm.F2 (816 ± 2 µm) exhibited the largest beads, followed by F1 (761 ± 5µm), n = 20. At the same time, F5, F4, F3, and F6 showed smaller beads gradually, with F6 being the smallest (Figure 7). The larger particle size observed in F2 indicated that bead size is not only determined by alginate content but also by the combined effect of polymer ratio and solution viscosity. The balanced alginate–gellan ratio in F2 may have improved the viscosity of the solution, resulting in slightly larger droplets than those in alginate-dominant F1. Formulation F5, which contains the same polymer composition as F2 but with a stronger cross-linker concentration (2% $AlCl_3$), produced large beads, indicating that the cross-linker concentration significantly influenced the formation of bead structures. Gellan-rich formulations F3 and F6 yielded smaller beads than the alginate-

dominant formulations, likely due to their tighter matrix formation and stronger intermolecular interactions, which limit droplet expansion during gelation.

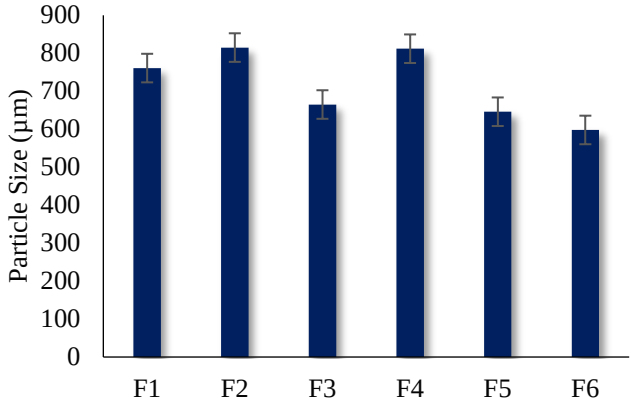

Figure 7: Average Particle Size of Prepared Microbeads

Percentage of Yield

The percentage yield of the formulations ranged between 75.79% and 92.15% (Figure 8). F4 provided the highest yield (92.15%), followed by F1 (91.27%). The lowest yield was obtained for F3 (75.79%). This difference may be observed due to the variation in polymer ratios and crosslinker concentrations. The highest yield values were obtained by F4 and F1, both of which are alginate-dominant. This phenomenon indicated that alginate-rich formulations offered better bead integrity. The lowest yield was achieved by F3 (75.79%), followed by F6 (77.21%). The lower yields of these two gellan-rich formulations may be attributed to weaker bead strength or partial fragmentation during processing. The balanced polymer ratios in F2 and F5 represented moderate matrix stability. Overall, it was found that the polymer composition highly influenced the bead formation and recovery efficiency in this formulation.

Swelling Index

The swelling index varied widely among formulations. The microbeads showed swelling index values ranging from 183% to 298% (Figure 8). Both the polymer ratio and crosslinking concentration contributed to the diversity in swelling among the 6 formulations. The formulations with alginate dominance showed a greater swelling capacity compared to the gellan-rich formulations, as the hydrophilic nature of alginate gum enhanced water uptake and expansion of the formulations. Simultaneously, formulations with similar polymer ratios, such as F1 vs. F4, F2 vs. F5, and F3 vs. F6, exhibited different swelling capacities due to variations in crosslinker concentration. Formulations with 2% $AlCl_3$ provided comparatively reduced swelling, suggesting that water penetration may be restricted due to the tighter network formation resulting from the higher crosslinker concentration. Hence, the highest swelling was observed in alginate-rich F1 (298%) with 1% $AlCl_3$, while the lowest was recorded for gellan-dominant F6 (183%) with 2% $AlCl_3$. In the case of F2, the balance ratio of polymer, as well as the lower concentration of cross-linking agent, displayed a greater extent of swelling capacity, i.e., 273%. Intermediate swelling was observed in F3 & F5, indicating the mutual effect of polymers & the crosslinker.

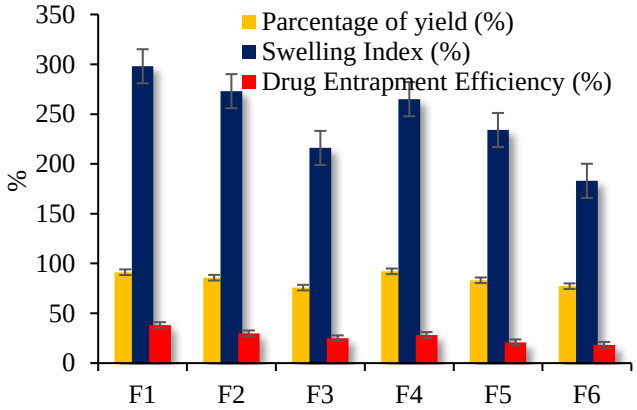

Figure 8: Percentage of yield, Swelling behaviour, and Drug Entrapment Efficiency of Valacyclovir microbeads

Drug Entrapment Efficiency

The entrapment efficiency of the drug varied significantly across the formulations, ranging from 18.37% to 38.19% (Figure 8). F1 retained the maximum amount of drug, and this superior performance of F1 is attributed to its hydrated and permeable matrix network. Due to the hydrophilic nature of alginate gum and a lesser amount of crosslinking agent, this formulation (F1) provided a favorable environment for drug incorporation during bead formation. Meanwhile, the least drug entrapment was obtained by F6 (18.37%) due to the higher gellan composition along with stronger crosslinking. This result confirmed that the rigid and less porous gel-forming nature of gellan was responsible for the more compact matrix formation, which reduced drug entrapment within the formulation. Again, the batches (F1–F3) showed better entrapment than the batches (F4–F6), suggesting that the higher crosslinker concentration significantly reduced entrapment efficiencies. Altogether, these observations indicated that alginate dominance supported entrapment, while gellan dominance and higher cross-linking limited it. The lower entrapment might be due to the strong crosslinking effect of aluminum chloride. Adjusting the polymer ratio or slightly reducing the crosslinker strength could help improve entrapment in future batches.

In vitro Release Study

The release study was conducted for 300 minutes for all batches. The highest cumulative drug release was achieved by F1 (53.75%), while the least drug release was obtained by F6 (35.20%). The drug release by the remaining batches was recorded between 40.12% and 49.05% (Figure 9). The release of the formulations was dependent on both the polymer composition and the concentration of the cross-linker. Due to its higher alginate content and lower cross-linking concentration, F1 created a much more permeable matrix network than the other formulations. This porous and loosely cross-linked gel network favored drug diffusion, resulting in the highest cumulative drug release. At the same time, F4, sharing the identical polymer proportion as F1, released a little less drug than F1. This behavior can be attributed to its higher crosslinker concentration, which produces a denser matrix network, while a higher proportion of alginate provides adequate hydration. The combined effect of gellan domination and stronger crosslinking caused F6 to release the lowest amount of drug throughout the same period, representing a comparatively rigid gel network with lower porosity. The intermediate release in F2 (44.04%), F5 (41.55%), and F3 (40.12%) demonstrated how the proportion of both gums, along with crosslinker level, balanced the drug diffusion and provided controlled but not maximal drug release.

Table 2: Drug release kinetics

Kinetic Model	Regression Coefficient						Mean
	F1	F2	F3	F4	F5	F6	
Zero Order	0.8009	0.7806	0.9576	0.9407	0.8073	0.9270	0.8690
First Order	0.8464	0.8177	0.9651	0.9443	0.8376	0.9370	0.8914
Higuchi	0.8368	0.8805	0.9842	0.9769	0.9015	0.9783	0.9264
Hixon-Crowell	0.8009	0.7806	0.9628	0.9514	0.8279	0.9338	0.8762
Korsymeyer-Peppas	0.8348	0.9360	0.9327	0.9245	0.9528	0.9396	0.9201
n	0.1245	0.1542	0.0868	0.1258	0.1402	0.1874	

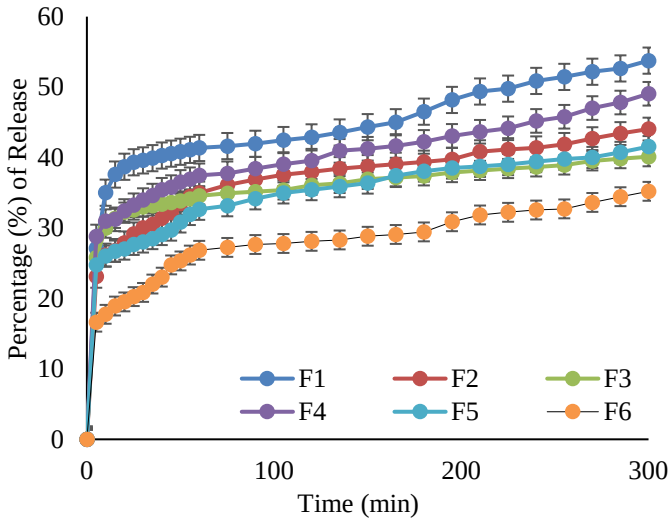

Figure 9: In-Vitro Comparison release study of prepared formulations

Drug Release Kinetics

Mechanistically, the prolonged drug release occurred primarily through Fickian diffusion, as indicated by the low release exponent (n = 0.08–0.18) and the strong correlation in the Higuchi model (R^2 = 0.9264). This suggests that both polymer relaxation and diffusion processes governed the release mechanism, consistent with prior work on hydrogel matrices. The regression coefficient exposed that F3 (R^2 = 0.9842), F6 (R^2 = 0.9783), and F4 (R^2 = 0.9769) followed the Higuchi model, signifying diffusion-controlled drug release. The Korsmeyer–Peppas model was best fitted for F2 (R^2 = 0.9360) and F5 (R^2 = 0.9528), whereas F1 did not exhibit a good correlation across all models, due to its high release rate (Table 2 and Figure 10).

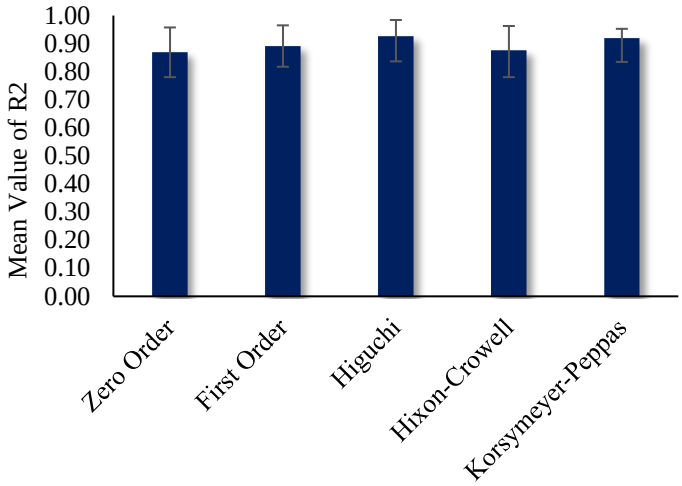

Figure 10: Comparison of Regression Coefficient of Release Kinetics

CONCLUSION

The present study successfully formulated and evaluated valacyclovir-loaded alginate–gellan microbeads using varying polymer ratios and crosslinking concentrations. FTIR confirmed drug–polymer compatibility. SEM images revealed spherical beads with a relatively smooth surface. Particle size, yield,

swelling index, entrapment efficiency, and release profiles were all strongly influenced by the balance between alginate and gellan, as well as crosslinker concentration. Among all batches, F1 exhibited the most favorable release behavior, whereas F6 showed the lowest. The developed microbeads provided sustained drug release for up to 300 minutes, indicating a controlled-release behavior suitable for improving the consistency of drug availability. The findings highlight the critical role of polymer composition and crosslink density in tailoring microbead performance, suggesting that careful optimization can enable controlled drug delivery. Overall, this approach offers a promising platform for oral delivery of valacyclovir. The prolonged release potential of these alginate–gellan microbeads is significant primarily in the therapeutic context of Valacyclovir. Due to Valacyclovir's short half-life, frequent administration is generally required, which can compromise patient adherence. By preparing a protective matrix that controls and slows the release of the drug, the microbeads help maintain therapeutic plasma concentrations for more extended periods, improve oral bioavailability, and reduce the frequency of dosing. This sustained-release approach has the potential to improve both treatment efficacy and patient compliance in antiviral therapy.

Future perspectives may emphasize the optimization of formulation using advanced design strategies, in vivo evaluation to establish pharmacokinetic and therapeutic benefits, stability studies under varied storage conditions, and commercial manufacturing. Furthermore, this delivery platform could be extended to other antiviral or poorly bioavailable drugs, thereby broadening its applicability in controlled drug delivery and offering advantages in patient convenience and therapeutic consistency.

FINANCIAL ASSISTANCE

NIL

CONFLICT OF INTEREST

The authors declare no conflict of interest.

AUTHOR CONTRIBUTION

Sudipta Das and Dipankar Saha designed and planned the study. Sankar Narayan Bhunia performed methodology, evaluation, data collection, and analysis. Rimi Dey and Sawan Das assisted in writing this paper. All authors contributed to the drafting of the manuscript and its review.

REFERENCES

[1] Khan Z, Abourehab MAS, Parveen N, Kohli K, Kesharwani P. Recent advances in microbeads-based drug delivery system for achieving controlled drug release. *J Biomater Sci Polym Ed*, **34(4)**, 541–564 (2023) https://doi.org/10.1080/09205063.2022.2127237.

[2] Lengyel M, Kállai-Szabó N, Antal V, Laki AJ, Antal I. Microparticles, microspheres, and microcapsules for advanced drug delivery. *Sci Pharm*, **87(3)**, 20 (2019) https://doi.org/10.3390/scipharm87030020.

[3] Jarvas G, Szerenyi D, Jankovics H, Vonderviszt F, Tovari J, Takacs L, et al. Microbead-based extracorporeal immuno-affinity virus capture: a feasibility study to address the SARS-CoV-2 pandemic. *Microchim Acta*, **190(3)**, 95 (2023) https://doi.org/10.1007/s00604-023-05671-9.

[4] Boi S, Rouatbi N, Dellacasa E, Di Lisa D, Bianchini P, Monticelli O, et al. Alginate microbeads with internal microvoids for the sustained release of drugs. *Int J Biol Macromol*, **156**, 454–461 (2020) https://doi.org/10.1016/j.ijbiomac.2020.04.083.

[5] Li H, Zhou J, Zhou Y, Dao J, Wei D, Wang Y. Advances in photocrosslinked natural hydrogel-based microspheres for bone repair. *J Polym Sci*, **62(22)**, 4966–4992 (2024) https://doi.org/10.1002/pol.20240302.

[6] Markovic M, Ben-Shabat S, Dahan A. Prodrugs for improved drug delivery: lessons learned from recently developed and marketed products. Pharmaceutics, **12(11)**, 1031 (2020) https://doi.org/10.3390/pharmaceutics12111031.

[7] Abdalla S, Briand C, Oualha M, Bendavid M, Béranger A, Benaboud S, et al. Population pharmacokinetics of intravenous and oral acyclovir and oral valacyclovir in pediatric population to optimize dosing regimens. Antimicrob Agents Chemother, **64(12)**, 01426-20 (2020) https://doi.org/10.1128/aac.01426-20.

[8] Das S, Samanta A, Das S, Nayak AK. Sustained release of acyclovir from alginate-gellan gum and alginate-xanthan gum microbeads. *JCIS Open*, **13**, 100106 (2024) https://doi.org/10.1016/j.jciso.2024.100106.

[9] Kurtulbaş E, Albarri R, Torun M, Şahin S. Encapsulation of Moringa oleifera leaf extract in chitosan-coated alginate microbeads produced by ionic gelation. *Food Biosci*, **50**, 102158 (2022) https://doi.org/10.1016/j.fbio.2022.102158.

[10] Dash S, Gutti P, Behera B, Mishra D. Anionic species from multivalent metal salts are differentially retained during aqueous ionic gelation of sodium alginate and could fine-tune the hydrogel properties. Int J Biol Macromol, **265**, 130767 (2024) https://doi.org/10.1016/j.ijbiomac.2024.130767.

[11] Yang D. Recent advances in hydrogels. *Chem Mater*, **34(5)**, 1987–1989 (2022) https://doi.org/10.1021/acs.chemmater.2c00188.

[12] Jana S, Pramanik R, Nayak AK, Sen KK. Gellan gum (GG)-based IPN microbeads for sustained drug release. *J Drug Deliv*

Sci Technol, **69**, 103034 (2022) https://doi.org/10.1016/j.jddst.2021.103034.

[13] Bhopte DK, Sagar R, Kori ML. Fabrication, optimization and characterization of floating microspheres of quinapril hydrochloride using factorial design method. Biomed Pharmacol J, **15(4)**, 2011–2024 (2022) https://doi.org/10.13005/bpj/2539.

[14] Khan HU, Nasir F, Maheen S, Shafqat SS, Shah S, Khames A, et al. Antibacterial and wound-healing activities of statistically optimized nitrofurazone- and lidocaine-loaded silica microspheres by the Box–Behnken design. Molecules, **27(8)**, 2532 (2022) https://doi.org/10.3390/molecules27082532.

[15] Wu MY, Kao IF, Fu CY, Yen SK. Effects of adding chitosan on drug entrapment efficiency and release duration for paclitaxel-loaded hydroxyapatite–gelatin composite microspheres. Pharmaceutics, **15(8)**, 2025 (2023) https://doi.org/10.3390/pharmaceutics15082025.

[16] Long T, Tan W, Tian X, Tang Z, Hu K, Ge L, et al. Gelatin/alginate-based microspheres with sphere-in-capsule structure for spatiotemporal manipulative drug release in gastrointestinal tract. Int J Biol Macromol, **226**, 485–495 (2023) https://doi.org/10.1016/j.ijbiomac.2022.12.040.

[17] Sharma Y, Mahar R, Chakraborty A, Nainwal N. Optimizing the formulation variables for encapsulation of linezolid into polycaprolactone inhalable microspheres using double emulsion solvent evaporation. Tuberculosis, **143**, 102417 (2023) https://doi.org/10.1016/j.tube.2023.102417.

[18] Frent OD, Duda-Seiman DM, Vicas LG, Duteanu N, Nemes NS, Pascu B, et al. Study of the influence of the excipients used for the synthesis of microspheres loaded with quercetin: their characterization and antimicrobial activity. Coatings, **13(8)**, 1376 (2023) https://doi.org/10.3390/coatings13081376.

[19] Frenț OD, Duteanu N, Teusdea AC, Ciocan S, Vicaș L, Jurca T, et al. Preparation and characterization of chitosan-alginate microspheres loaded with quercetin. *Polymers*, **14(3)**, 490 (2022) https://doi.org/10.3390/polym14030490.

[20] Mundarinti SHB, Ahad HA. Impact of Pistacia lentiscus plant gum on particle size and swelling index in central composite designed amoxycillin trihydrate mucoadhesive microspheres. *Indian J Pharm Educ Res*, **57**, 763–772 (2023) https://doi.org/10.5530/ijper.57.3.93.

[21] Nandee R, Chowdhury MA, Hossain N, Rana MM, Mobarak MH, Khandaker MR. Surface topography and surface morphology of graphene nanocomposite by FESEM, EDX and AFM analysis. *Nano-Structures & Nano-Objects*, **38**, 101170 (2024) https://doi.org/10.1016/j.nanoso.2023.101170.

[22] Xing L, Ding J, Chen D, Xiong C, Huang T, Xiong Z. Regulation of the surface morphology of microspheres by polymers with different crystallinities. *New J Chem*, **49(10)**, 4050–4060 (2025) https://doi.org/10.1039/D4NJ05113K.

[23] Dobhal K, Verma S, Singh A, Kukreti G. Fabrication and evaluation of floating zidovudine microbeads for prolonged kinetic release and bioavailability. *Indian Journal of Pharmaceutical Education and Research*, **59(1)**, 65–73 (2024) https://doi.org/10.5530/ijper.20254139.

[24] Das S, Dey R. Trivalent ion cross-linked and acetalated gellan gum microspheres of glimepiride. *Asian J Pharm Clin Res*, **13(5)**, 66–68 (2020) https://doi.org/10.22159/ajpcr.2020.v13i5.37229.

[25] Giotopoulou I, Stamatis H, Barkoula NM. Encapsulation of thymol in ethyl cellulose-based microspheres and evaluation of its sustained release for food applications. Polymers, **16(23)**, 3396 (2024) https://doi.org/10.3390/polym16233396.

[26] Roy D, Das S, Samanta A. Design and in vitro release kinetics of liposomal formulation of acyclovir. *Int J Appl Pharm*, **11(6)**, 61–65 (2019) https://doi.org/10.22159/ijap.2019v11i6.34917.

[27] Andaririt DR, Purnaningtyas SRD, Wijayanto A. Validation of the UV-Vis spectrophotometric method for the determination of ascorbic acid content in beverage preparations based on a standard vitamin C calibration curve. *Open Access Health Scientific Journal*, **6(2)**, 249–257 (2025) https://doi.org/10.55700/oahsj.v6i2.101.

[28] Mallick A, Sahu R, Nandi G, Dua TK, Shaw TK, Dhar A, et al. Development of liposomal formulation for controlled delivery of valacyclovir: an in vitro study. *J Pharm Innov*, **18(3)**, 1020–1029 (2023) https://doi.org/10.1007/s12247-022-09706-1.

[29] Mishra A, Sinha VR, Sharma S, Mathew AT, Kumar R, Yadav AK. Molecular and qualitative characterization of compatibility between valacyclovir hydrochloride and excipients as raw materials for the development of solid oral dosage formulation. *American Journal of Biopharmacy and Pharmaceutical Sciences*, **3(1)**, 8–18 (2023) https://doi.org/10.25259/AJBPS_12_2023.

[30] Thombare N, Mahto A, Singh D, Chowdhury AR, Ansari MF. Comparative FTIR characterization of various natural gums: a criterion for their identification. *J Polym Environ*, **31(8)**, 3372–3380 (2023) https://doi.org/10.1007/s10924-023-02821-1.